Received 22 May 2025
Revised 23 June 2025
Accepted 25 June 2025

Validity range of a quasi-static method for adjusting the pre-sag of simple railway catenary systems

Bastian Schick, Zhendong Liu and Sebastian Stichel
Department of Engineering Mechanics, KTH Royal Institute of Technology, Stockholm, Sweden

Abstract

Purpose – Adding an appropriate pre-sag to the geometry of simple catenary systems for electric railways can improve their performance in dynamic interaction with the pantographs of trains operating under them. The value of pre-sag can be obtained by empirical approximation or computationally expensive optimisation. This study aims to define a simple but accurate method to determine a suitable pre-sag without dynamic simulations and to find its limitations.

Design/methodology/approach – A quasi-static method to determine the ideal value of pre-sag is described based on elasticity variations. It considers variations of the static contact force. The limits of this method are investigated by comparing it to a parametric dynamic simulation study. In the dynamic simulation, an optimal level of pre-sag is identified for each contact force level. The influence of the speed in the dynamic simulation results is expressed in two parameters: the quasi-static influence in the mean contact force and the dynamic influence in the ratio between the vehicle speed and the wave propagation speed in the contact wire.

Findings – The comparison between the suggested method and the dynamic simulations shows a high consistency up to a speed limit of around 40 % of the wave propagation speed. The best agreement with the dynamic results is achieved by calculating the optimal pre-sag based on the absolute elasticity variation.

Practical implications – The simplified approach for determining the pre-sag is valid for low-speed applications, such as suburban railway lines. For these cases, a highly suitable geometry can be obtained with the suggested method, meaning a significantly reduced computational effort. As a case study for this work, the results are applied to a Swedish suburban rail line upgrade case.

Originality/value – The static uplift force is added as a varied parameter in dynamic simulations. The shift in system behaviour from low to high dynamics is described, and how the benefits from pre-sag are visible and then disappear. The limit value of the low-dynamics regime is identified to be 40 %.

Keywords Pantograph, Overhead catenary line, Dynamic interaction, Energy supply infrastructure, Wave propagation speed, Suburban rail

Paper type Research article

1. Introduction

When designing overhead catenary lines (OCLs) for electric railways, it is crucial to ensure good dynamic interaction between the OCL and the trains operating in contact with them. A well-adjusted contact force with limited dynamic variations should always be ensured to guarantee an adequate power supply whilst avoiding excessive wear loads on the structure. For making design choices, engineers rely on standardised design rules and empirical equations as guidelines for design (Puschmann *et al.*, 2024). In addition, the latest simulation tools allow extensive parametric studies to be performed to find optimal designs (Bruni, Bucca, Carnevale, Collina, & Facchinetti, 2018, 2025; Wu *et al.*, 2022), and to ensure compliance with international guidelines such as the European Technical Specifications for

Railway Sciences
Vol. 4 No. 4, 2025
pp. 522-535
Emerald Publishing Limited
e-ISSN: 2755-0915
p-ISSN: 2755-0907
DOI 10.1108/RS-05-2025-0016

Funding: We thank Trafikförvaltningen Region Stockholm and Trafikverket for funding and supporting this study.

Interoperability (TSI) (European Commission, 2014). The OCL systems for DC operation are subject to higher demands than AC systems, as their low voltage and high currents in the power transfer make them sensitive to contact quality. Therefore, higher static contact forces are used in DC operation (European Commission, 2014).

Introducing a pre-sag, as shown in Figure 1, aims to compensate for the effects of the varying elasticity between the stiffer support at the masts and the free mid-span of the OCL. Adjusting the pre-sag to match the expected difference in uplift would ideally eliminate the pantograph oscillations at the wavelength of one span. In practice, dynamic effects complicate the interaction. Even though the general concept of pre-sag application is well established in the literature, the application limits are not clearly defined. Adding stitch wires at the masts is a common way of reducing elasticity variations (Puschmann *et al.*, 2024). This study, however, focuses on simple OCL system designs without stitch wires.

Since the introduction of computational methods to evaluate the interaction between pantograph and catenary systems, there have been approaches to verify or optimise the choice of pre-sag in catenary designs by simulation (Gostling & Hobbs, 1983). Early studies have been restricted to giving indications about a specific unfavourable case (Nordstrøm Jensen & True, 1998) or picking the best out of a limited number of options (Zhang, Mei, & Zeng, 2002). More extensive parametric studies have become feasible with increasing computational and modelling capabilities. A typical approach for such a parametric study has been to simulate the dynamic interaction for different pre-sag levels and a range of speeds (Cho, Lee, Park, Kang, & Kim, 2010; Mei & Song, 2022). One study (Gregori, Tur, Nadal, & Fuenmayor, 2018) adopted an algorithm to optimise the pre-sag geometry on an individual dropper level, including adapting their longitudinal position to a specific speed and mean contact force. The results show considerable possible improvements whilst indicating trade-off situations. Complex optimised geometries, however, also increase the complexity of implementation. In (Gil *et al.*, 2024), an optimisation approach for application on a real railway line is described. All studies have in common that a higher density of studied parameter constellations allows the detection of patterns. Based on that, ranges of applicability or allowable operational parameters can be identified. The consideration of operation with multiple pantographs and critical sections further complicates the optimisation (Harèll, Drugge, & Reijm, 2005; Liu, Jönsson, Stichel, & Rønnquist, 2016; Pombo, Antunes, & Ambrósio, 2012; Xu, Song, & Liu, 2020; Yao, Yang,

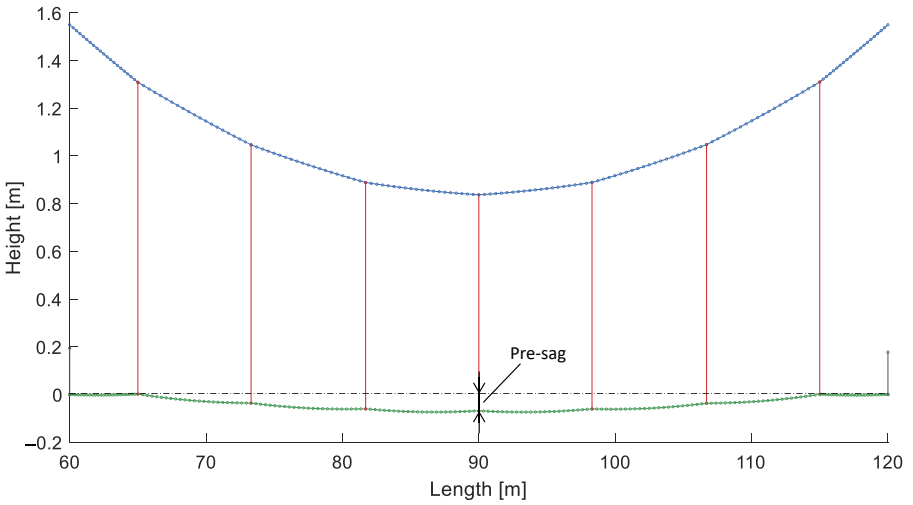

Figure 1. Lateral view of a simple catenary's geometry with applied pre-sag. Source: Authors' own work

Wang, & Zhang, 2022, 2025). The recommendations in the literature can be generalised as a range of pre-sag of below 0.5 to 2 ‰ of the span length. The recommended pre-sag for stitched high-speed systems is low (Kwon, Cho, Lee, & Oh, 2016; Mei & Song, 2022). In contrast, the performance of simple OCL systems can be improved considerably by adjusting the pre-sag, especially for low speeds (Cho, 2008; Cho *et al.*, 2010; Nåvik, Rønnquist, & Stichel, 2016). The applied pre-sag in currently implemented systems reflects many of the mentioned findings (Puschmann *et al.*, 2024; Vo Van, Massat, Laurent, & Balmes, 2014).

This work relates to the findings summarised above by defining a simple but specific method for engineering adjustments based on well-known principles. Chapter 4 presents a quasi-static calculation method based on the nonlinear contact force-dependent catenary elasticity to calculate a suitable pre-sag value. The adjusted pre-sag can be applied to standardised design geometries for low to medium-speed applications by changing the maximum value along the pre-sag curve along the span. The results of the given case study are presented in Chapter 5, together with a series of transient dynamic simulations to verify the method and determine its validity range. The simulations include the static contact force as a systematically varied parameter. This extends existing studies and enables the study of the correlation of pre-sag and contact force for the ideal interaction between the pantograph and the OCL system. The used simulation tool and the studied case for application are described in chapters 2 and 3, respectively.

2. Simulation tool description

This study uses the finite element (FE)-based simulation tool CaPaSIM (Jönsson, Stichel, & Nilsson, 2015). This tool successfully participated in the simulation benchmark 2015 (Bruni *et al.*, 2015), and its 3D version is continuously being developed and validated (Schick, Liu, & Stichel, 2022). The tool uses the ANSYS software for FE calculations and has been equipped with automated parametric options that allow detailed adjustments in the model setup. For this study, the messenger wire is modelled with link elements and the contact wire is modelled with Euler˛–Bernoulli beam elements. The droppers are modelled as links with tension-only cable characteristics. The model explicitly represents the steady arms as links between the contact wire support points and a fixed boundary, as indicated in Figure 2. All catenary sections included in this study are modelled with straight track alignment and the full lateral stagger. The initial mesh geometry is calculated analytically using a linearised mechanical equilibrium, including the intended pre-sag. The elements are scaled to a maximal length of 0.5 m in the longitudinal direction. The importance of correct alignment of the catenary structure, especially the contact wire for dynamic simulation, has been emphasised in literature and

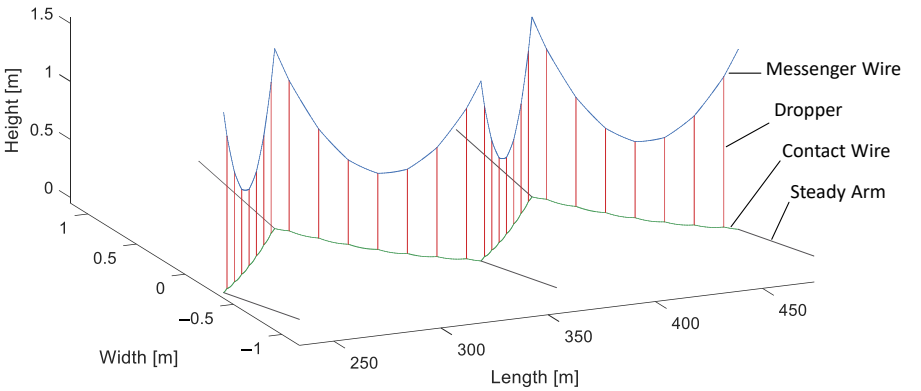

Figure 2. 3D view of catenary geometry with the alignment of finite elements. Source: Authors' own work

methods to ensure this are presented (Antunes, Ambrósio, & Pombo, 2016; Arnold & Simeon, 2000; Lopez-Garcia, Carnicero, & Torres, 2006; Song, Liu, Rønnquist, Nåvik, & Liu, 2020; Tur, García, Baeza, & Fuenmayor, 2014). Before the dynamic simulation, CaPaSIM performs a series of iterative static simulations for each catenary section, in which the geometry is verified and adjusted similarly to (Cho *et al.*, 2010). In addition to adjusting the dropper lengths via the messenger wire nodes, this procedure includes adjusting the wire tensions by setting an initial strain. It also adjusts the steady arm fixture locations to ensure the correct alignment of the contact wire in vertical and lateral directions. When deviations are below a predefined tolerance, the elasticity is calculated, and the corrected structure is used for the dynamic simulations. The Newmark method is used for time integration with a time step of 2 ms. In this study, structural damping is applied with a relative damping ratio of 0.02, and a numerical damping ratio of 0.005 is applied through the integration coefficients.

A lumped mass-spring representation of a pantograph type commonly used in Sweden is used to model the pantograph. This model consists of two lumped mass layers, where a spring-damper combination supports the upper layer, whereas the lower layer is supported by damping and friction elements. The exact pantograph parameters can be found in Table 4 in the Appendix. The contact between the pantograph and the catenary is modelled using the penalty method with a contact stiffness of 50 kN/m.

3. Case study description

This study is performed in the context of an existing DC OCL system upgrade on the Swedish suburban line Saltsjöbanan. The system parameters are summarised in Tables 2 and 3 in the Appendix. The objective of the upgrade is to fulfil the TSI norm for 1,5 kV DC systems (European Commission, 2014), which necessitates a significant increase in static contact force according to EN 50318 (CENELEC, 2018). The infrastructure owner aims to investigate adjustments of the catenary structure parameters, including pre-sag geometry, for a new range of mean contact forces and to retain as much of the existing wires and support structures as possible. Sweden has no national standardised DC systems, as all main lines are electrified with 15 kV AC systems. The geometry and characteristics of the original OCL infrastructure are derived from the Swedish AC system type ST 7,1/7,1. The dynamic interaction quality is quantified in the standard deviation of the contact force σ and its ratio to the mean contact force F_m metrics follow EN 50367. The maximum uplift of the contact wire at the mast supported by the steady arms should not exceed half of the possible uplift movement, as they do not have a built-in uplift stop. For larger uplifts, there is a risk of collision. This maximal allowable uplift Δy_{StA} is 83.5 mm in the given case. The TSI lift force requirement for 1,5 kV DC systems, defining maximal static contact force F_{stat} of 140 N, can only be fulfilled if the tension force T of the contact and messenger wire is increased above the original 7.1 kN. As the closest reference, the existing Swedish AC OCL system type ST 9,8/9,8 was chosen as a basis for the geometry and characteristics of the suggested upgrade. The existing infrastructure has already been adapted to DC operation by using a heavier contact wire with a cross-section of 120 mm^2, which is reused. The actual span lengths vary significantly within each catenary section of the actual catenary layout of the studied line. Therefore, a representative section of the track has been modelled in addition to the ideal section with identical spans of maximal span length. The representative section consists of 31 spans with a total length of 1340.2 m. The span lengths for this section range from 24.7 to 58.4 m. The exact span length composition can be found in Table 5 in the Appendix. The curve radii are not considered for the representative section, as the catenary geometry is modelled straight. An essential characteristic of catenary systems in curves is the variation of the elasticities at the masts from span to span, depending on the wire angles at the steady arm. The model indirectly represents this effect due to the inconsistent change of span lengths and the resulting variation of lateral drag force at the steady arms. The elasticity of the catenary is affected by the ratio of the lateral and vertical forces acting on the steady arm.

4. Method

Two variants of a simplified calculation method for pre-sag adjustment are evaluated against the results of a parametric simulation study. This calculation method is introduced in section 4.1 after re-stating the underlying empirical approximations as a baseline. The calculation method is based on the variation of the elasticity of the catenary system obtained from static simulations. A quasi-static perspective is taken by studying the expected speed-dependent mean contact force, including aerodynamics and considering the nonlinear contact force-dependent elasticity of the catenary system.

4.1 A quasi-static method for calculating a suitable pre-sag

Following the basic principle of compensating the difference in uplift along a span due to the elasticity variation, the sag can be chosen based on the used F_{stat} on the pantographs of the vehicle fleet. For a system with contact wire tension T_{CW} and messenger wire tension T_{MW}, the elasticity at mid-span e_{mid} for a span of length l can be approximated by the empirical rule

$$e_{mid} = \frac{l}{k(T_{CW} + T_{MW})} \tag{1}$$

where the constant factor k is approximated to 4 in simple catenary systems (Puschmann *et al.*, 2024). The desirable level of pre-sag S (in mm or S_{rel} in ‰ of l) can then be based on the difference in elasticity at the mast e_{mast}. For this simplified approach, e_{mast} is commonly approximated to be 30 to 50 % of e_{mid} (Puschmann *et al.*, 2024).

$$S = F_{stat}(e_{mid} - e_{mast}) \tag{2}$$

$$S_{rel} = F_{stat}(e_{mid} - e_{mast})/l \tag{3}$$

S_{rel} relates to the usual proportional definition of pre-sag. In Swedish span design regulations, the applied pre-sag is always proportional to the span length. A more accurate representation of the catenary elasticity can be obtained from static simulations performed with the FE model by applying a point load in the vertical direction on the contact wire and then measuring the resulting uplift Δy. The result obtained from such a study on the nonlinear elasticity of the OCL structure is shown in Figure 3, considering contact force variations leading to dropper unloading. The computational effort for such simulations is considerably lower than running dynamic simulations. This example shows that the changes in the elasticity pattern are small and most prominent in the region around the droppers next to the mast. Therefore, a small number of simulations, such as three force steps of 50 N, are sufficient to capture them. The expected error from not considering force dependence in the elasticity pattern will be estimated in section 5.1.

The effect of changes to the pre-sag on elasticity has also been studied. For the same dropper placement, the results in Figure 4 show that an increase in pre-sag leads to no notable change to the elasticity pattern for low contact forces. However, the sensitivity to higher contact force increases around the mast and decreases at the mid-span for a higher pre-sag. This means that in a span with higher pre-sag, the elasticity increases slower for higher forces at the mast and faster for higher forces at mid-span. This further decreases the effect of large contact forces on the elasticity variation along one span. At this point, it can be assumed that it is sufficient to run a single set of static simulations using a value of S as a geometry input that is estimated based on Equations (1) and (2). This will be confirmed in section 5.1 as well.

To estimate the ideal pre-sag from a quasi-static perspective, the expected mean uplift contact force F_m is calculated from F_{stat}, the aerodynamic lift coefficient α_{ae} and the vehicle speed v (in km/h) as

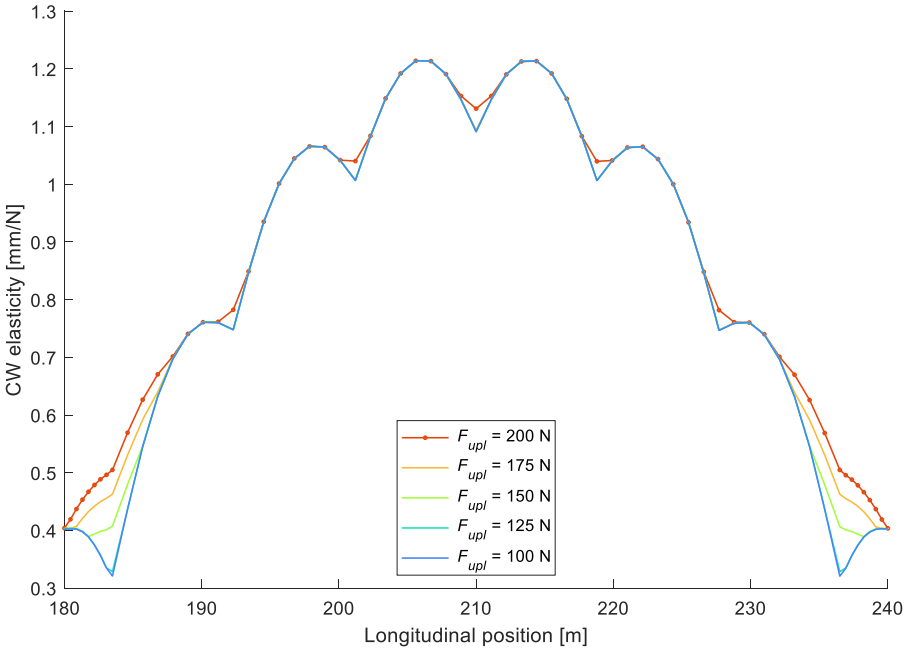

Figure 3. Static catenary elasticity of the system type ST 7,1/7,1 along one standard span for different contact forces. Source: Authors' own work

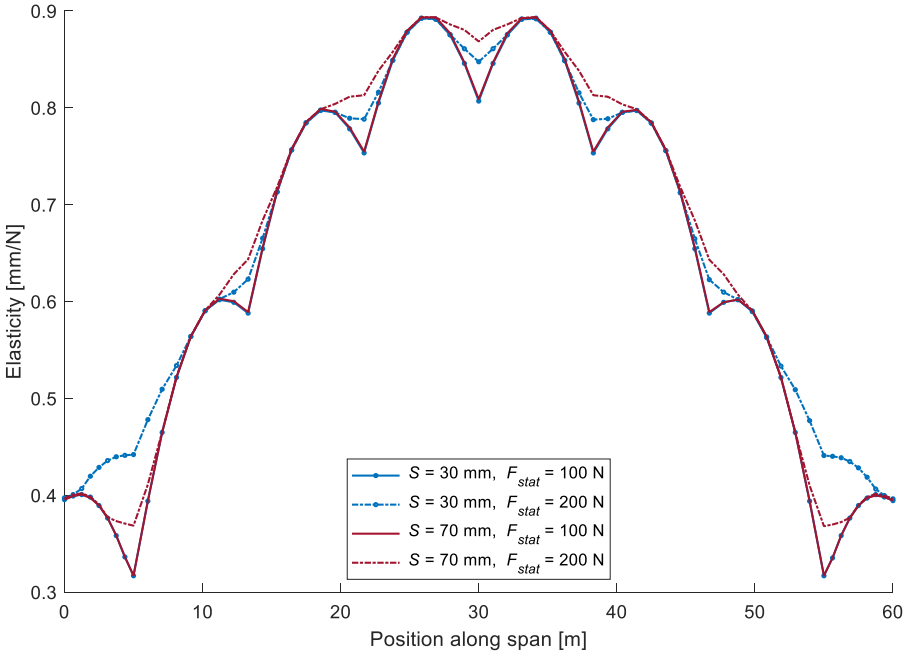

Figure 4. Comparison of the static catenary elasticity of the ST 9,8/9,8 system for different applied pre-sag levels and contact forces along one standard span. Source: Authors' own work

$$F_m = F_{stat} + \alpha_{ae} v^2. \quad (4)$$

Based on EN 50367, values of F_m between 70 and 179 N can be expected for 1,5 kV DC systems. The elasticity curve for each operation case can be obtained by interpolating between the two curves from the static simulation with the closest forces to F_m. From the interpolated elasticity at the expected F_m, it is possible to determine the expected uplift variation. Therefore, the recommended pre-sag can be calculated using Equation (2) but using F_m and the exact values for e_{mast} and e_{mid}. Knowing the entire elasticity curve opens up for a second more accurate option calculating a suitable pre-sag. This variant uses the maximal and the minimal values of e along the span, which is also used for calculating the degree of elasticity uniformity defined in the literature (Puschmann *et al.*, 2024).

$$S = F_m(e_{max} - e_{min}) = F_m \Delta e \quad (5)$$

5. Results

The results of the empirical and quasi-static approaches are presented and compared in section 5.1. Section 5.2 adds the dynamic simulation results to the comparison to study if the quasi-static description is sufficient and at which speed the influence of dynamic effects becomes too large. That is where the applicability limit of the quasi-static approach is reached. In section 5.3, the identified patterns in the dynamic simulation results are related to existing expressions for optimal pre-sag considering dynamic effects.

5.1 Estimation and quasi-static calculation

As a reference for comparison, the empirical approximation of the desirable pre-sag level is calculated using Equation (1). Assuming a F_{stat} of 140 N, we obtain the values in Table 1 for the two systems studied in the case example. The lower sag values result from the assumption of $e_{mast} = 0.5\, e_{mid}$, whereas the higher values result from $e_{mast} = 0.3\, e_{mid}$. The possible range of values agrees with the general design principle of applying 0.5 to 2 ‰ of pre-sag on simple catenary systems for low speed. A more specific design recommendation can be obtained from the quasi-static calculation method described in section 4.1. Table 2 shows the resulting

Table 1. Approximated pre-sag levels are based on empirical rules

	Approximation - $S = F_{stat}(e_{mid} - e_{mast})$		
Tension T [kN]	Estimated elasticity e_{mid} [mm/N]	Pre-sag S [mm]	Pre-sag S_{rel} in ‰ of l
7.1/7.1	1.056	74–104	1.23–1.73
9.8/9.8	0.765	54–75	0.90–1.25

Source(s): Table created by authors

Table 2. Exact pre-sag levels are calculated using simulated elasticity curves

	$S = F_m(e_{mid} - e_{mast})$		$S = F_m(e_{max} - e_{min})$	
Tension T [kN]	Pre-sag S [mm]	Pre-sag S_{rel} in ‰ of l	Pre-sag S [mm]	Pre-sag S_{rel} in ‰ of l
7.1/7.1	96	1.69	118	1.96
9.8/9.8	58	0.96	79	1.32

Source(s): Table created by authors

pre-sag values for a F_m of 140 N. The values in the left-hand columns are calculated using e_{mid} and e_{mast}, whereas the right-hand values are calculated using e_{max} and e_{min}. Comparing those results shows that the pre-sag values based on the absolute elasticity difference are even higher than the upper end of the estimated range.

The calculations are extended to a broader range of values to study the effect of varying F_m, as shown in Figure 5a). The results for ideal spans are calculated from a section of identical 60 m spans, whereas the results for mixed spans are a mean value based on the representative catenary section mentioned in Section 3. The relative pre-sag is calculated individually per span and then averaged for the entire section. For a F_m of up to 150 N, there is a strictly linear dependency between F_m and the pre-sag due to the unchanged elasticity. Around 150 N, the nonlinear behaviour of the elasticity sets in, and the curves start to flatten out slightly. Again, using the absolute elasticity difference along one span, as indicated with the dashed lines, generally gives larger values of desirable pre-sag than using only the mast and mid-span points. This becomes evident from local minima and maxima in elasticity along the span, which increase the maximal difference, especially for low contact forces. The elasticity variation would be slightly reduced for higher contact forces, resulting in a somewhat smaller ideal pre-sag. Not considering this elasticity change due to the higher contact force leads to an error that increases with the difference of contact force to the value used in the elasticity simulation. Figure 5b) shows that the relative error can get as high as 16 % when calculating the ideal pre-sag for homogeneous spans for an F_m of 179 N using the elasticity curve for 100 N. This error is significantly decreased again when considering the effect of a larger pre-sag on the elasticity. Using the elasticity curve for the close-to-optimal pre-sag S of 70 mm instead of the nominal 30 mm, the error at F_m of 179 N is reduced to only 2 % when using the elasticity curve for 100 N. A single elasticity curve is therefore sufficient.

5.2 Verification by dynamic simulation

A series of dynamic simulations is performed to verify the calculated ideal pre-sag levels. They are performed on the OCL system variant with the higher wire tensions derived from the ST 9,8/9,8 system. The studied parameters are pre-sag level S in a range between 30 and 70 mm with 10 mm steps, vehicle speed v between 50 and 180 km/h with 10 to 20 km/h steps and static contact force F_{stat} between 50 and 155 N with 15 N steps. All possible parameter combinations are simulated, adding up to 400 simulation instances. The results are presented in terms of

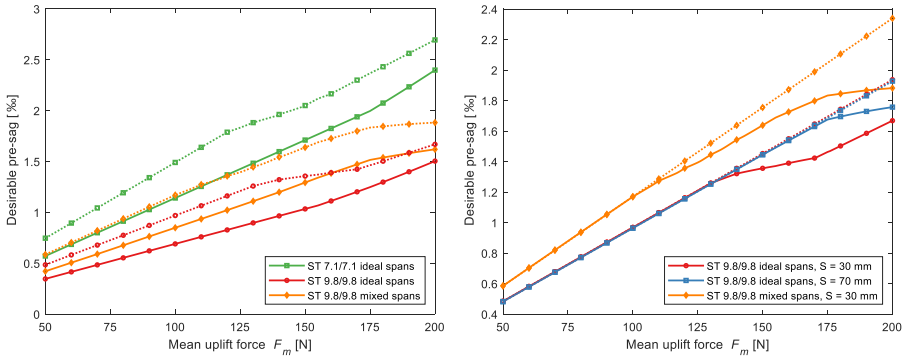

(a) **(b)**

Figure 5. Calculated ideal pre-sag S dependent on F_m for different systems and span configurations. In (a), the solid lines use elasticity at the mast and mid-span, whilst the dotted lines use maximal and minimal elasticity. In (b), only maximal and minimal elasticity is used. The solid lines are calculated using interpolation of several elasticity curves, whereas only the elasticity curve for F_m of 100 N is used for the dotted lines. Source: Authors' own work

mean contact force F_m for consistency with the previous quasi-static analysis. In addition, the dynamic contribution of the gradually increased speed is indicated in terms of the dimensionless factor β, which describes the vehicle speed v proportion to the wave propagation speed in the contact wire c_{CW}. β is calculated as

$$\beta = \frac{v}{c_{CW}} = \frac{v}{\sqrt{T_{cw}/\rho_{CW}}} \tag{6}$$

where ρ_{CW} indicates the mass per metre of the wire (Dahlberg, 2006). This approach aims to introduce comparable metrics that allow the separation of the quasi-static and dynamic effects and to evaluate how they affect the pantograph–catenary interaction concerning the applied pre-sag S. The comparison is made to the dynamic results of the ideal section.

The results are plotted in layers representing the relative speed levels to visualise them in one graph. Figure 6 shows the standard deviation ratio σ/F_m dependent on F_m, where each subfigure represents one value of S and each line shows a relative speed β. As long as there is a distinct minimum in σ/F_m, the corresponding value of F_m can be concluded to be the optimal value for this S, and that the applied pre-sag has a beneficial effect on the dynamic interaction. This beneficial effect is most pronounced at low speeds. It becomes less distinct towards a β of 0.35 and entirely disappears at 0.41. Another effect of the increased relative speed is that the optimal range of F_m is slightly shifting with increased β. This observation will be studied further in the next section.

In Figure 7, the perspective is shifted, and a separate graph is plotted for each relative speed level. This allows a comparison of the dynamic results to the calculated ideal quasi-static pre-sag level from Figure 5. The comparison shows that the calculation approach based on e_{max} and e_{min} fits well into the optimal range of σ for β under 0.4. For the speeds resulting in a β above 0.4, the beneficial effects disappear and the linear relationship no longer matches the

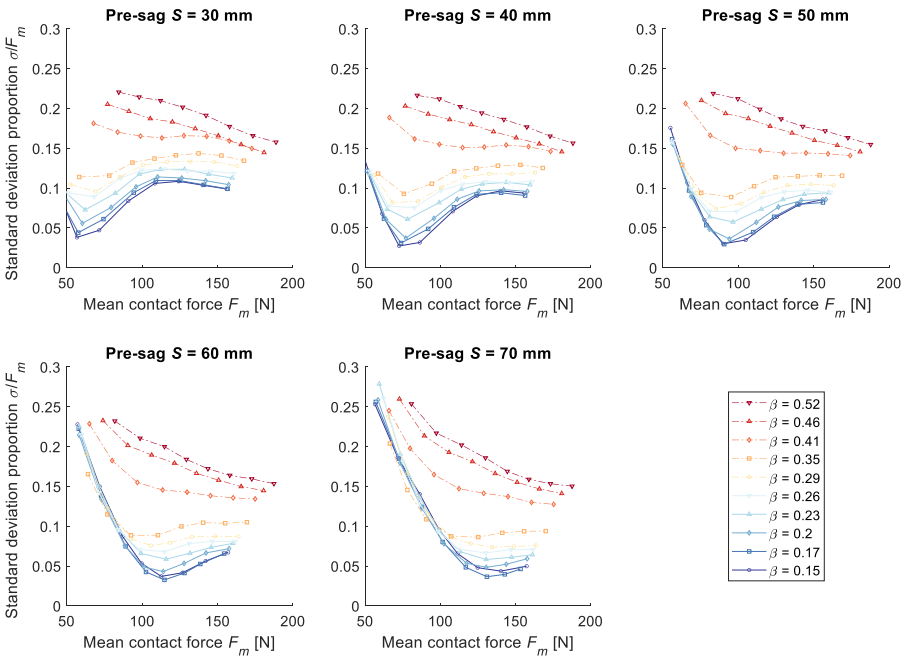

Figure 6. Contact force standard deviation σ over F_m ratio, dependent on F_m, β and S. Source: Authors' own work

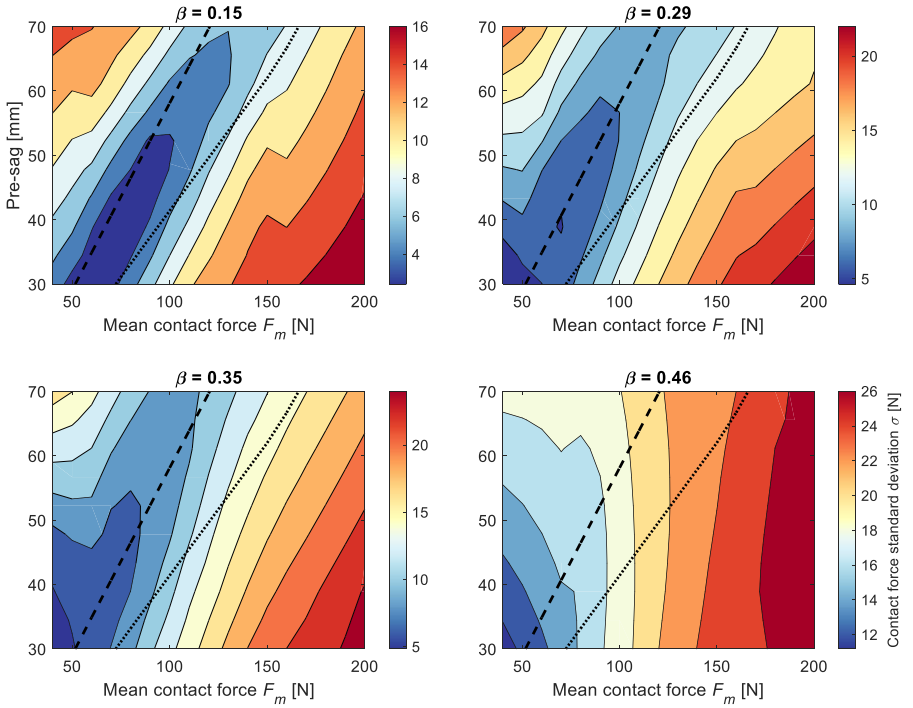

Figure 7. Comparison of quasi-static estimation of optimal pre-sag S with dynamic simulation results. The dotted trend lines show the values based on e_{mast} and e_{mid}, and the dashed lines show values based on Δe. Source: Authors' own work

simulation results. Therefore, choosing the pre-sag S based on quasi-static calculations using the expected range of F_m is reliable as long as the operational speeds are below the limit of 40 % of c_{CW}. In the case study described here, the maximum relative speed β is 0.26, so the quasi-static method is suitable. The resulting S_{rel} from the quasi-static evaluation is not strictly linearly dependent on the span length, as shown in Figure 5. Nevertheless, they are summarised in relative terms here to give a general design guideline. The values for an expected range of F_m between 70 and 148 N, based on a F_{stat} of 70–140 N and speeds up to 90 km/h are 0.68 to 1.35 ‰ for the ideal spans and 0.82 to 1.62 ‰ for the mixed spans. Taking a mean value of that, the recommended S_{rel} is determined to be 1.12 ‰, which corresponds to 67 mm for the nominal spans with a length l of 60 m. If the expected range of F_m could be narrowed down, the recommended S_{rel} would change accordingly. It should, however, be noted that the increase in pre-sag also makes the pantograph–OCL couple sensitive to too low levels of F_m, which implies high requirements on the proper calibration of F_{stat} and requires an increase of F_{stat} for the existing vehicle fleet. As seen in the curves for low speed in Figure 6, a higher S causes a substantial rise in σ over F_m. Even though all values are below the limit of 0.3, the most critical cases are those where a low F_m is combined with an excessive S.

The effect of the pre-sag S on the maximum uplift of the contact wire at the support $\Delta y_{StA,max}$ is also investigated. Based on section 4.1, it is expected that $\Delta y_{StA,max}$ would slightly decrease with the increase of S. This effect can be observed in the dynamic simulation results, it is however comparatively small.

5.3 Influence of speed on the optimal pre-sag

In this section, the shift in the optimal relation between S and F_m due to increased β will be investigated in detail. The ultimate goal of such an analysis is to find a general expression, including β. The influence of β could, for example, be estimated as an empirical dynamic correction factor with coefficients k and a such as

$$S_{dyn} = S_{stat} + k\beta^a. \tag{7}$$

As noted in the previous section, there are optimal values of F_m which give a minimal σ/F_m for respective S. The change of these values with the increase of β is plotted in Figure 8. The minimum σ/F_m values are derived from spline interpolation of the curves shown in Figure 6. It can be observed that the optimal values decrease or remain constant. A decrease implies that for a given F_m, the optimal S_{dyn} increases with increasing β. This can be associated with a dynamic amplification of the uplift effect but stands in direct conflict with findings in other research (Cho *et al.*, 2010; Mei & Song, 2022; Puschmann *et al.*, 2024), which generally indicate that the optimal sag for high speeds is small to non-existent. However, the trend curves do not show any optimal values for higher β. This leads to the assumption that the optimal values for the higher speeds either lie outside the parametric range studied here or that there is an abrupt shift from the static to the dynamic regime around $\beta = 0.4$ and that no explicit trend can be drawn between these two regimes. An extension of the studied parametric range could shed further light on this assumption.

5.4 Discussion

As mentioned above, there has been an attempt in (Cho *et al.*, 2010) to derive a general equation that considers the speed for calculating an ideal pre-sag level S_{dyn}. This equation was, however, based on a simplified model representation of the catenary, and its primary purpose was to show the influence of different parameters on S_{dyn}. In that equation, it was suggested that S_{dyn} is inversely proportional to v^2. Comparing the equation in (Cho *et al.*, 2010) to the dynamic simulation results presented here, it can be noted that this proportionality cannot replicate the observed patterns. Values of S_{dyn} calculated with that equation agree well with the optima found by simulation in this study at speeds around 70 to 80 km/h. For higher speeds, those calculated values decrease however much faster than the ones found by simulation here.

The generality of the good agreement between calculation and simulation in the quasi-static regime should be further verified by assessing the sensitivity to the specific characteristics of the pantograph and catenary type couple, especially regarding the definition of a speed limit

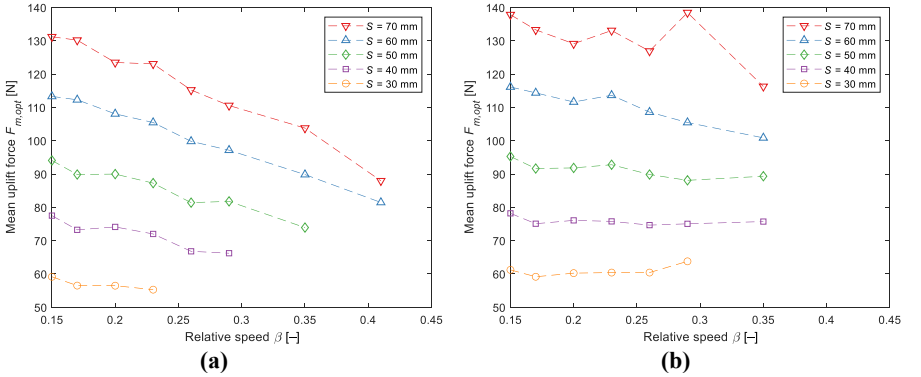

Figure 8. Trend of optimal F_m for different S in relation to β. In (a), the absolute minima of σ are used, whereas (b) shows the minima of σ/F_m. Source: Authors' own work

for the applicability of the quasi-static regime. A systematic study on the implications of the operation with multiple pantographs would also be a good addition to the present results to ensure that a beneficial effect of the pre-sag even is maintained, even though it would be uncommon in the studied line. For application in suburban lines with small track radii, is important to ensure that the effects of the curve and stagger variations on elasticity are properly taken into consideration. This should include compensation of rail cant effects by sag adjustment.

6. Conclusions

This work presented a quasi-static method for calculating a suitable pre-sag for simple catenary systems based on their nonlinear elasticity and the mean contact force. A high consistency was found between the quasi-static approximation using the difference between maximal and minimal elasticity Δe and transient dynamic simulations within a specific speed range. Therefore, this approach is a suitable option with low computation effort for cases within the quasi-static regime. Based on the presented results, the quasi-static approach can be assumed to be applicable up to 40 % of the wave propagation speed in the contact wire c_{CW}. This percentage is commonly exceeded in mainline traffic, but is applicable for suburban railways.

Based on the observed patterns in the dynamic simulation results, trend lines for optimal constellations considering the relative speed were studied. They show that none of the equations proposed so far can fully capture the patterns and that further studies are required. For these studies, the parametric range should be extended to higher speeds and lower pre-sag values. Then, an extension of the validity above 40 % of the wave propagation speed and an application on high-speed operation could be possible. An application of the same calculation method on catenaries with stitch wires is possible; its accuracy should be proven in a separate study.

For the presented case study with low speeds and high contact force, it was observed that contact force dynamics are not the limiting factor in such conditions. Instead, the choice of parameters must fulfil the limitation of the maximal allowable uplift $\Delta y_{StA,max}$. This means that the maximal acceptable static contact force F_{stat} is purely defined by uplift compatibility, which should be verified by field measurements. Adding pre-sag to the catenary geometry can improve contact dynamics but only slightly reduce $\Delta y_{StA,max}$. Therefore, it should be seen as a means to improve operational characteristics within a feasible setup, not a solution to use an otherwise inadequate setup.

It was also shown that determining an optimal level of pre-sag S is prone to overfitting when optimising for a too-narrow scope of parameter values. Sensitivities and possible deviations in the operational parameters should be considered for the choice of S to ensure the beneficial effects of the adjustments in the system. The assembly and maintenance tolerances should, for example, be set within the width of the beneficial ranges of S.

Supplementary material

The supplementary material for this article can be found online.

References

Antunes, P., Ambrósio, J., & Pombo, J. (2016). Catenary finite element model initialization using optimization. *Civil-Comp Proceedings*, *110*. doi: 10.4203/ccp.110.106.

Arnold, M., & Simeon, B. (2000). Pantograph and catenary dynamics: A benchmark problem and its numerical solution. *Applied Numerical Mathematics*, *34*(4), 345–362. doi: 10.1016/S0168-9274(99)00038-0.

Bruni, S., Ambrósio, J., Carnicero, A., Cho, Y. H., Finner, L., Ikeda, M., … Zhang, W. (2015). The results of the pantograph–catenary interaction benchmark. *Vehicle System Dynamics*, *53*(3), 412–435. doi: 10.1080/00423114.2014.953183.

Bruni, S., Bucca, G., Carnevale, M., Collina, A., & Facchinetti, A. (2018). Pantograph–catenary interaction: Recent achievements and future research challenges. *International Journal of Rail Transportation*, *6*(2), 57–82. doi: 10.1080/23248378.2017.1400156.

Bruni, S., Bucca, G., Facchinetti, A., Gregori, S., & Pombo, J. (2025). Recent developments on pantograph-overhead line interaction. *Vehicle System Dynamics*, *1–37*(7), 1358–1394. doi: 10.1080/00423114.2025.2484453.

CENELEC. (2018). Railway applications – Current collection systems – Validation of simulation of the dynamic interaction between pantograph and overhead contact line (EN 50318). CENELEC.

Cho, Y. H. (2008). Numerical simulation of the dynamic responses of railway overhead contact lines to a moving pantograph, considering a nonlinear dropper. *Journal of Sound and Vibration*, *315*(3), 433–454. doi: 10.1016/j.jsv.2008.02.024.

Cho, Y. H., Lee, K., Park, Y., Kang, B., & Kim, K. N. (2010). Influence of contact wire pre-sag on the dynamics of pantograph–railway catenary. *International Journal of Mechanical Sciences*, *52* (11), 1471–1490. doi: 10.1016/J.IJMECSCI.2010.04.002.

Dahlberg, T. (2006). Moving force on an axially loaded beam - with applications to a railway overhead contact wire. *Vehicle System Dynamics*, *44*(8), 631–644. doi: 10.1080/00423110500165523.

European Commission (2014). *Commission Regulation (EU) No 1301/2014 of 18 November 2014 on the technical specifications for interoperability relating to the 'energy' subsystem of the rail system in the Union*. The European Commission.

Gil, J., Song, Y., Gregori, S., Tur, M., Rønnquist, A., & Fuenmayor, F. J. (2024). Railway catenary optimisation with span variability by an iterative optimisation algorithm for large numbers of parameters. *Engineering Structures*, *299*, 117090. doi: 10.1016/J.ENGSTRUCT.2023.117090.

Gostling, R. J., & Hobbs, A. E. W. (1983). The interaction of pantograph and overhead equipment: Practical applications of a new theoretical method. *Proceedings of the Institution of Mechanical Engineers - Part C: Journal of Mechanical Engineering Science*, *197*(1), 61–69. doi: 10.1243/PIME_PROC_1983_197_077_02.

Gregori, S., Tur, M., Nadal, E., & Fuenmayor, F. J. (2018). An approach to geometric optimisation of railway catenaries. *Vehicle System Dynamics*, *56*(8), 1162–1186. doi: 10.1080/00423114.2017.1407434.

Harèll, P., Drugge, L., & Reijm, M. (2005). Study of critical sections in catenary systems during multiple pantograph operation. *Proceedings of the Institution of Mechanical Engineers, Part F: Journal of Rail and Rapid Transit*, *219*(4), 203–211. doi: 10.1243/095440905X8934.

Jönsson, P. A., Stichel, S., & Nilsson, C. (2015). CaPaSIM statement of methods. *Vehicle System Dynamics*, *53*(3), 341–346. doi: 10.1080/00423114.2014.999799.

Kwon, S. Y., Cho, Y. H., Lee, K., & Oh, H. K. (2016). Simulation and testing of the effect of current collection performance according to pre-sag in 400km/h overhead contact lines. *Journal of the Korean Society for Railway*, *19*(3), 288–296. doi: 10.7782/JKSR.2016.19.3.288.

Liu, Z., Jönsson, P. A., Stichel, S., & Rønnquist, A. (2016). Implications of the operation of multiple pantographs on the soft catenary systems in Sweden. *Proceedings of the Institution of Mechanical Engineers, Part F: Journal of Rail and Rapid Transit*, *230*(3), 971–983. doi: 10.1177/0954409714559317.

Lopez-Garcia, O., Carnicero, A., & Torres, V. (2006). Computation of the initial equilibrium of railway overheads based on the catenary equation. *Engineering Structures*, *28*(10), 1387–1394. doi: 10.1016/J.ENGSTRUCT.2006.01.007.

Mei, G., & Song, Y. (2022). Effect of overhead contact line pre-sag on the interaction performance with a pantograph in electrified railways. *Energies*, *15*(6875), 6875. doi: 10.3390/en15196875.

Nåvik, P., Rønnquist, A., & Stichel, S. (2016). The use of dynamic response to evaluate and improve the optimization of existing soft railway catenary systems for higher speeds. *Proceedings of the*

Institution of Mechanical Engineers, Part F: Journal of Rail and Rapid Transit, *230*(4), 1388–1396. doi: 10.1177/0954409715605140.

Nordstrøm Jensen, C., & True, H. (1998). Dynamics of an electrical overhead line system and moving pantographs. *Vehicle System Dynamics*, *29*(sup1), 104–113. doi: 10.1080/00423119808969555.

Pombo, J., Antunes, P., & Ambrósio, J. (2012). A study on multiple pantograph operations for high-speed catenary contact. *Civil-Comp Proceedings*, *99*(January). doi: 10.4203/ccp.99.139.

Puschmann, R., Schmieder, A., Dölling, A., Braun, W., Mielsch, F., Altmann, M., & Ullmann, H. (2024). *Fahrleitungen elektischer Bahnen. Planung, Berechnung, Ausführung, Betrieb* (4th ed). Druck+Verlg Ernst Vögel GmbH.

Schick, B., Liu, Z., & Stichel, S. (2022). Modelling of pantograph-catenary interaction around critical speed. In *Proceedings of The Fifth International Conference on Railway Technology: Research, Development and Maintenance* (Vol. 1, pp. 1–7). doi: 10.4203/ccc.1.4.12.

Song, Y., Liu, Z., Rønnquist, A., Nåvik, P., & Liu, Z. (2020). Contact wire irregularity stochastics and effect on high-speed railway pantograph-catenary interactions. *IEEE Transactions on Instrumentation and Measurement*, *69*(10), 8196–8206. doi: 10.1109/TIM.2020.2987457.

Tur, M., García, E., Baeza, L., & Fuenmayor, F. J. (2014). A 3D absolute nodal coordinate finite element model to compute the initial configuration of a railway catenary. *Engineering Structures*, *71*, 234–243. doi: 10.1016/j.engstruct.2014.04.015.

Vo Van, O., Massat, J. P., Laurent, C., & Balmes, E. (2014). Introduction of variability into pantograph–catenary dynamic simulations. *Vehicle System Dynamics*, *52*(10), 1254–1269. doi: 10.1080/00423114.2014.922199.

Wu, G., Dong, K., Xu, Z., Xiao, S., Wei, W., Chen, H., . . . Huang, Z. (2022). Pantograph – catenary electrical contact system of high - speed railways : Recent progress , challenges , and outlooks. In *Railway Engineering Science*. Singapore: Springer Nature. doi: 10.1007/s40534-022-00281-2.

Xu, Z., Song, Y., & Liu, Z. (2020). Effective measures to improve current collection quality for double pantographs and catenary based on wave propagation analysis. *IEEE Transactions on Vehicular Technology*, *69*(6), 6299–6309. doi: 10.1109/TVT.2020.2985382.

Yao, Y., Yang, Z., Wang, J., & Zhang, W. (2022). Analysis of contact force and uplift of pantograph–catenary system in overlap section based on numerical simulations and experimental tests. *Vehicle System Dynamics*, *61*(10), 1–24. doi: 10.1080/00423114.2022.2117056.

Yao, Y., Wang, J., Yang, J., Yang, Z., Wang, W., Wang, B., & Mu, M. (2025). Research on optimisation of overlapping section of catenary based on simulation and line testing. *Vehicle System Dynamics*, 1–26. doi: 10.1080/00423114.2025.2477835.

Zhang, W., Mei, G., & Zeng, J. (2002). A study of pantograph/catenary system dynamics with influence of presag and irregularity of contact wire. *Vehicle System Dynamics*, *37*(SUPPL.), 593–604. doi: 10.1080/00423114.2002.11666265.

Corresponding author
Bastian Schick can be contacted at: bschick@kth.se

Bastian Schick is a PhD student at KTH Royal Institute of Technology in Stockholm, Sweden. His studies focus on numerical simulations of pantograph-catenary interaction. He is applying these to the dynamic characterisation related to realistic operational conditions and catenary variations, as well as wear prediction and pantograph modelling. He has a master's degree in Rail Vehicle Engineering from KTH. His other fields of work are brake systems and longitudinal dynamics of long freight trains. He won the Shift2Rail Innovation Awards 2021 Student Competition with his Master's Thesis on Pneumatic Modelling of Long Freight Trains.